Nanotechnology **20** (2009) 085706 (6pp) doi:10.1088/0957-4484/20/8/085706

Nanoscale characterization of isolated individual type I collagen fibrils: polarization and piezoelectricity

Majid Minary-Jolandan and Min-Feng Yu

Department of Mechanical Science and Engineering, University of Illinois at Urbana-Champaign, 1206 West Green Street, Urbana, IL 61801, USA

E-mail: mfyu@uiuc.edu

Received 28 August 2008, in final form 10 December 2008
Published 3 February 2009
Online at stacks.iop.org/Nano/20/085706

Abstract

Piezoresponse force microscopy was applied to directly study individual type I collagen fibrils with diameters of ∼100 nm isolated from bovine Achilles tendon. It was revealed that single collagen fibrils behave predominantly as shear piezoelectric materials with a piezoelectric coefficient on the order of 1 pm V^{-1}, and have unipolar axial polarization throughout their entire length. It was estimated that, under reasonable shear load conditions, the fibrils were capable of generating an electric potential up to tens of millivolts. The result substantiates the nanoscale origin of piezoelectricity in bone and tendons, and implies also the potential importance of the shear load-transfer mechanism, which has been the principle basis of the nanoscale mechanics model of collagen, in mechanoelectric transduction in bone.

1. Introduction

It has been a long-held concept that a number of biological materials, such as bone, skin and connective tissues such as tendon, show piezoelectric behavior similar to that of certain crystalline materials [1–3]. The first scientific observation of the piezoelectric effect in biological tissues dates back to 1941 [3, 4]. It has been suggested that a cross-linked uniaxial system of well-ordered and asymmetric fibrous molecules, capable of being polarized in response to a shear stress, is responsible for this effect in biological materials [3]. It has further been postulated that the piezoelectric charges produced under stress in such materials may stimulate cellular response and thus the growth and healing of these tissues [5–8]. The piezoelectric effect in bone has been suggested as the cause for the Wolff's law, which states the ability of bone to remodel itself under different load conditions [6], albeit the direct experimental proof of that is still elusive.

Bone at the nanoscale is a composite composed of hydroxyapatite (HA) nanocrystals (∼65% in mass) and collagen fibrils (∼35%) [8, 9]. The centro-symmetric crystal structure of HA excludes it to be piezoelectric [8, 10], and in fact, it is has been shown that after decollagenation of bone no piezoelectric effect is observed [11]. The major contributor to the piezoelectricity in bone is therefore the collagen. There are more than fourteen types of collagen and the most studied one is the type I collagen [12]. This fibrous collagen is found in bone, teeth, ligament, and tendon [12, 13]. Accordingly, piezoelectricity has been studied in bone, skin, teeth, and tendon extensively [1–3, 14]. Piezoelectric coefficient values on the order of $d_{14} \sim 2$ pm V^{-1} and $d_{15} \sim 1$ pm V^{-1} were reported for tendons [2, 15] and $d_{14} \sim 0.1$ pm V^{-1} for collagen films [16]. d_{13} and d_{33} in tendons were found to be negligibly small [2]. d_{14} values directly measured from bone samples were also small, on the order of ∼0.2 pm V^{-1} [2, 15], and from dentin and enamel in human tooth, in the range of ∼0.03–2.5 pm V^{-1} [17–19]. However, due to the existence of varying percentage of collagen and different orientation of collagen fibrils in such macroscopic samples [8], extracting quantitative information about the piezoelectric response of a single collagen fibril is not straightforward. On the other hand, owing to the hierarchical structure of collagen, their importance as the most abundant structural protein in mammals and as a major constituent of all extracellular matrices, and their numerous developmental and physiological functions [3, 12, 20], to find their electromechanical properties at the nanoscale is highly desirable.

In this paper we probe piezoelectricity of individual type I collagen fibrils having diameters on the order of 100 nm with piezoresponse force microscopy (PFM) [14, 21, 22]. PFM is a

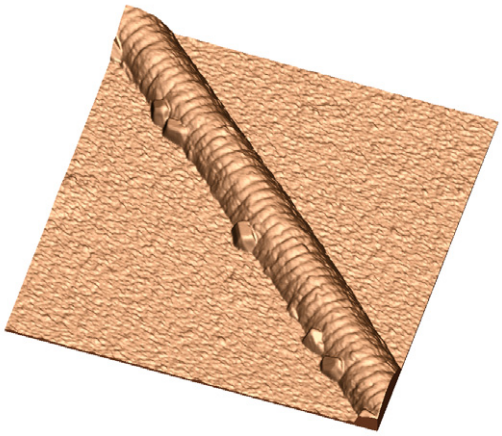

Figure 1. AFM tapping mode amplitude image of a collagen fibril with ∼100 nm in diameter (scan size: 2 μm). A few salt nanocrystals remain along the edge of the fibril.

(This figure is in colour only in the electronic version)

demonstrated technique based on scanning probe microscopy that allows the nanoscale characterization of the converse piezoelectric property of material of interest with extremely high sensitivity and spatial resolution [21–24]. PFM operated in both vertical and lateral response modes was applied to examine the piezoelectric responses of isolated individual collagen fibrils along both their radial and axial directions, and to determine the polarization direction in such fibrils.

2. Materials and methods

2.1. Sample preparation

Type I collagen extracted from bovine Achilles tendon (Sigma-Aldrich) was used throughout the study. About 10 mg of the extracts was swollen in 20 ml of 0.01 M sulfuric acid over night. The resulting solution was shred by a blender for ∼10 min at 0 °C temperature followed by 30 min of sonication [25]. Different dilutions were made by adding the required amount of phosphate buffer saline (PBS) solution. A Si chip coated with a thin gold layer was dipped in the final dispersion for about an hour to collect collagen fibrils. The collagen fibril-coated substrate was then rinsed several times with deionized water to wash off the precipitated salt crystals of PBS and was dried at room temperature.

2.2. PFM imaging and measurement

Throughout the experiment, Pt-coated atomic force microscope (AFM) probes with a nominal bending stiffness of $k_b \sim 0.15$ N m^{-1}, a torsional stiffness of $k_t \sim 40$ N m^{-1} and a resonance frequency of ∼12 kHz were used (MikroMasch USA, CA). A Dimension 3100 AFM equipped with a signal access module, an external lock-in amplifier (Signal Recovery Model 5210), and a function generator (Stanford Research System DS 340) was used for PFM measurement. Humidity was controlled at ∼12% during the experiment. First, individual collagen fibrils were imaged in tapping mode

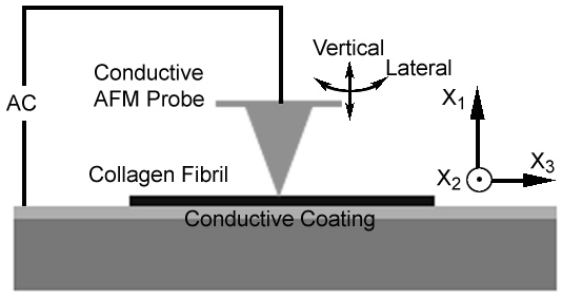

Figure 2. Schematics showing the general PFM experimental set-up, and the coordinate system assigned to describe the system.

AFM, and fibrils with typical periodic banding structures were identified (figure 1). AFM was then switched to the contact mode for PFM measurement. Two operation modes of PFM, the vertical response mode and the lateral response mode, were used to study the piezoelectric responses in collagen fibrils. The vertical response mode PFM measures the local vertical (out-of-plane) deformation of a collagen fibril by monitoring the deflection signal of AFM probe cantilever. The lateral response mode PFM measures the local shear (in-plane) deformation by monitoring the torsional twist of AFM probe cantilever. In both modes, a harmonic AC voltage signal of 10 kHz was applied between the AFM probe and the grounded conductive substrate. The modulated piezoelectric response from a collagen fibril resulted from the converse piezoelectric effect was then measured with a lock-in amplifier. Figure 2 depicts the general experimental set-up and the coordinate system used in the study. Particularly for the lateral response mode PFM measurement, the substrate was rotated prior to the experiment to align the long axis of the studied fibril perpendicularly or parallel to the long axis of the AFM cantilever in order to study the in-plane shear piezoelectric deformation along the axial (along the X_3 direction) or the radial direction (along the X_2 direction), respectively. Both PFM image mapping and single point measurements were carried out. PFM image mapping of the acquired piezoresponse amplitude and phase signals over collagen fibrils was obtained by scanning across a region of interest with a scanning rate of 0.1 Hz. For the single point measurement, AFM probe tip was positioned and engaged on top of the central axis of a collagen fibril before the measurement. In all measurements, the contact force during the PFM measurement was kept below ∼2.5 nN. Based on the mechanical analysis assuming an elliptical Hertzian contact between the AFM probe tip and the cylindrical collagen fibril, the indentation into collagen fibril is estimated to be less than 1 nm. (A separate dynamic nanoindentation study, not included in this paper, confirms that the indentation deformation of such collagen fibrils under such forces is much less than 1 nm.)

2.3. PFM sensitivity calibration

To quantitatively evaluate the acquired piezoelectric responses from collagen fibrils, the sensitivities of the AFM system operated in the vertical and the lateral response PFM modes

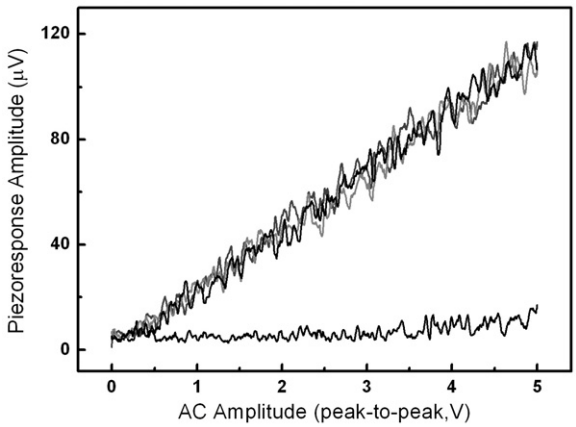

Figure 3. Three overlapping shear piezoresponse versus AC peak-to-peak amplitude curves acquired with the lateral response mode PFM at the same location on a collagen fibril showing the linear piezoelectric response. Included also in the lower portion of the panel is the curve acquired at the same location showing the response due to electrostatic and electrostrictive interactions.

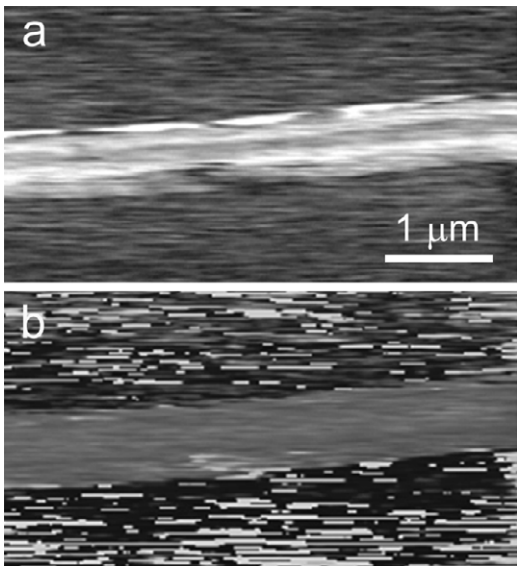

Figure 4. Piezoresponse amplitude (a) and phase (b) images taken with the lateral response mode PFM from a collagen fibril on a Au-coated Si substrate.

were calibrated. The out-of-plane deflection sensitivity was calibrated based on the standard analysis of the force curve acquired from pressing the AFM probe on a hard substrate. This out-of-plane deflection sensitivity was measured to be ∼5.7 mV nm^{-1}. The in-plane torsional twist sensitivity was calculated based on the geometry of the AFM probe and the measured out-of-plane deflection sensitivity. $R = 2L/3h$, where R is the in-plane/out-of-plane sensitivity ratio, $h = 25\ \mu$m is the height of the AFM tip and $L = 460\ \mu$m is the length of the cantilever [26, 27]. For the AFM probes used in this study, $R \sim 12$, which yields an in-plane torsional twist sensitivity of ∼70 mV nm^{-1}.

3. Results and discussion

3.1. PFM measurement of individual collagen fibrils

Figure 3 shows the shear piezoelectric response of a collagen fibril (∼80 nm in diameter) measured with the lateral response mode PFM. The shear deformation along the axial (X_3) direction increases linearly with the increasing amplitude of the applied AC voltage signal, reflecting the piezoelectric nature of the electromechanical coupling (the first-order coupling) in the collagen fibril. The three overlapping responses shown in figure 3 were acquired from the same local point on the collagen fibril, demonstrating the reproducibility of the response. The slope of the line in figure 3 is ∼22 μV/V_{pp} (or ∼44 μV V^{-1}). Based on the in-plane torsional twist sensitivity of the cantilever (∼70 mV nm^{-1}), the effective shear piezoelectric coefficient, d_{15}, calculated directly from the slope of the acquired curve, is 0.6 pm V^{-1}. (This value will be more accurately determined later in the discussion.) Included also in figure 3 is a response curve acquired from the same local point on the collagen fibril when the reference signal for the lock-in amplifier is set at two times the frequency of the applied AC voltage signal. Since the electrostatic signal is proportional to square of the amplitude of the applied AC voltage ($\propto V^2 \sim \sin^2(\omega t) \sim \sin(2\omega t)$), the response reflects mainly the electrostatic interaction and the electrostrictive coupling (the second-order electromechanical coupling) involved in the measurement [28, 29]. The response is comparatively negligible. In additional PFM measurements, no clear vertical piezoelectric response was observed along the X_1 direction and no shear piezoelectric response along the X_2 direction from this and other collagen fibrils.

The piezoelectric nature of individual collagen fibrils was also clearly revealed in the acquired piezoresponse amplitude and phase images. Figure 4 shows the piezoresponse amplitude and piezoresponse phase images taken with the lateral response mode PFM from scanning a collagen fibril on a Au-coated substrate. Clearly resolved and uniform piezoresponse amplitude signal on the collage fibril distinguished the noisy and small signal on the substrate, so did the piezoresponse phase signal acquired simultaneously from the same region. Particularly, the piezoresponse phase signal was related to the axial polarization in collagen fibril. Physically rotating a collagen fibril by 180° caused a 180° change of the acquired piezoresponse phase signal, as shown in figure 5. This axial polarization was further found to be unipolar based on examining the piezoresponse phase signals on 17 sample locations along a long collagen fibril of ∼100 μm in length, including its two ends (data not shown). More interestingly, a phase signal line scan across two adjacent end segments of a looped collagen fibril clearly showed a 180° phase change (figure 5(c)), as a result of the unipolar nature of individual collagen fibrils.

3.2. Structural origin of piezoelectricity in collagen

In order to elucidate the origin of piezoelectricity in a collagen fibril, its internal structure and molecular organization should be discussed. Tropocollagen or collagen molecule, as the

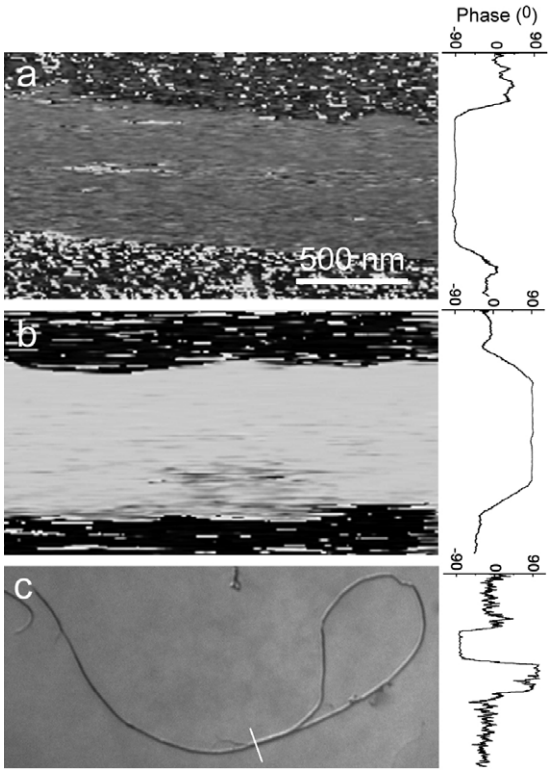

Figure 5. Piezoresponse phase image and the corresponding line scan phase signal across a collagen fibril before (a) and after (b) physically rotating the fibril by 180°. (c) Optical microscope image showing a naturally looped collagen fibril on a substrate and the corresponding line scan phase signal taken with the lateral response mode PFM across the marked line in the image, showing a phase difference of 180°.

structural subunit of collagen fibril, consists of three left-handed polypeptide helixes (α chains) wrapped around one another in a right-handed fashion [12, 13]. A distinctive feature of collagen is the arrangement of amino acids in each collagen subunit. Each α chain is composed of a series of triplet sequence Gly–X–Y, where X and Y are often proline and hydroxyproline [12, 13, 20]. Glycine (Gly), as the smallest amino acid, has only one hydrogen atom as side chain pointing into the center of the triple helix and is repeated every third amino acid in the sequence. Proline and hydroxyproline, having a ring in their amino acid structure, give rise to the rigidity and stability of the triple helix structure [12, 13]. Hydrogen bonds stabilize three chains together [13].

Each collagen molecule is ~300 nm in length and ~1.5 nm in diameter and has two ends, COOH terminal (or the C terminal) and NH_2 terminal (or the N terminal) [12, 13, 30]. To form a fibril, molecules associate laterally by covalent bonds [13, 20] in a fashion that each molecule is displaced one quarter of its length ($D \sim 67$ nm) in respect to the adjacent molecule (this quarter stagger arrangement is shown in figure 6). Such an arrangement produces a gap zone and an overlap zone which in an AFM image appear as discrete bands (figure 1). The covalent cross-links are formed in the overlap region between the carbonyl groups and other amino acids of adjoining molecules (mostly lysine and hydroxyl-lysine). Insolubility of collagen fibrils is believed to be due to these covalent cross-links [12, 20, 31]. It is suggested that these covalent cross-links create a networked rope structure in a collagen fibril and enable the molecules to transmit mechanical forces to the neighboring molecules [31, 32].

Recent electron density map data reveal that crystallographic superlattice of collagen is formed of quasihexagonally packed collagen molecules [31]. The fact that collagen fibril exhibits only shear piezoelectric response can be explained by its (semi-)hexagonal symmetry structure. For this symmetry group, C_6, the converse piezoelectric effect is described by [2, 33]:

$$\begin{pmatrix} \varepsilon_{11} \\ \varepsilon_{22} \\ \varepsilon_{33} \\ 2\varepsilon_{23} \\ 2\varepsilon_{13} \\ 2\varepsilon_{12} \end{pmatrix} = \begin{pmatrix} 0 & 0 & d_{13} \\ 0 & 0 & d_{31} \\ 0 & 0 & d_{33} \\ d_{14} & d_{15} & 0 \\ d_{15} & -d_{14} & 0 \\ 0 & 0 & 0 \end{pmatrix} \begin{pmatrix} E_1 \\ E_2 \\ E_3 \end{pmatrix}, \qquad (1)$$

according to the coordinates defined in figure 2. In PFM, E_2 and E_3 represent the lateral components of the applied electric field between the AFM tip and the substrate, and are symmetric fields. E_1 represent the vertical electric field underneath the AFM tip. The symmetric fields of E_2 and E_3 do not induce overall deformation (or the torsional motion of the cantilever), so $\varepsilon_{33} = \varepsilon_{22} = 0$. The vertical response was negligible according to our measurement with the vertical response mode PFM, so $\varepsilon_{11} \sim 0$. Therefore, the only nonzero strain elements are ε_{13} and ε_{23}. The torsional motion of AFM cantilever in the lateral response mode PFM measures only the in-plane shear, ε_{13}, and accordingly, $2\varepsilon_{13} = d_{15}E_1 - d_{14}E_2$. Considering that E_2 under an AFM tip is a symmetric field (so the induced shear piezoresponses cancel themselves), only d_{15} contributes to the acquired shear piezoresponse, so $d_{15} = 2\varepsilon_{13}/E_1$.

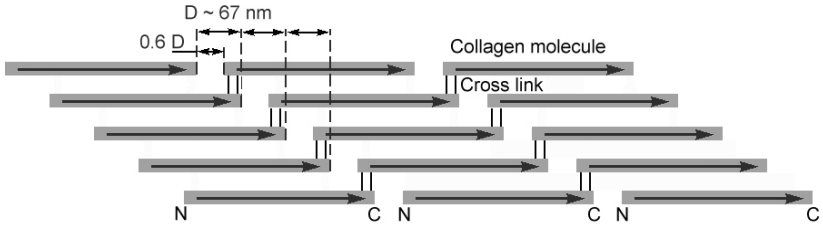

Figure 6. Structure of a collagen fibril: the quarter stagger arrangement, the polarization and the intermolecular covalent cross-links.

3.3. Determination of shear piezoelectric constant

We applied a two-dimensional finite element model to examine the shear piezoelectric response in a collagen fibril. According to the linear piezoelectric theory, the strain field (ε) produced due to the inverse piezoelectric effect is related solely to the applied electric field (E) according to $\varepsilon_{ij} = d_{ijk}E_k$, where d is the piezoelectric tensor and is an independent property of material. In the modeling, we attempt to find the appropriate d to match the measured displacement (thus the local strain) underneath the AFM tip. The AFM tip was modeled as a half circle of 50 nm in radius in contact with the top surface of a cylindrical collagen fibril having a diameter of 100 nm, and was biased at a particular voltage relative to the substrate. Surrounding the collagen fibril was air with a dielectric constant of $\varepsilon_{\text{air}} = 1$. The dielectric constant for the collagen fibril was assumed to be isotropic and was ∼5 [34], see also the note in[1]. The electric field distribution was then simulated using the finite element program, ANSYS. In the meantime, the displacement and strain distributions in the collagen fibril due to the piezoelectric effect were also simulated, assuming the fibril as an isotropic elastic material with an elastic modulus E of 5 GPa, a Poisson ratio ν of 0.5 and a shear modulus $G = E/2(1 + \nu)$ [8, 35] (the mechanical properties of collagen actually have no bearing in our following estimate of piezoelectric constant, as we fit only the strain field directly based on the piezoelectric strain-electric field equation). The interaction volume between the AFM probe tip and the collagen fibril in the PFM measurement was dependent on the applied voltage and the dielectric properties of collagen [18]. When a collagen fibril was subjected to a 2.5 V bias applied from the AFM tip, the interaction volume was found to be on the order of the tip radius (∼50 nm) [36], and the electric field in the interaction volume was on the order of $\sim 4 \times 10^7$ V m^{-1}. By fitting the modeled shear deformation underneath the AFM tip with the measured deformation of ∼1.5 pm at a tip bias of 2.5 V from our PFM measurement, we found that the collagen fibril developed a maximum strain on the order of $\gamma_{13} = 2\varepsilon_{13} \sim 5 \times 10^{-5}$ due to the piezoelectric effect, and from which the value of d_{15} was found to be ∼1 pm V^{-1} (or pC N^{-1}) for the collagen fibril.

3.4. Electric potential generation within collagen fibrils

It has been suggested that at the nanoscale the main deformation mechanism of bone involves the shearing of mineral matrix with respect to collagen fibrils [37, 38]. As mentioned earlier, this shear deformation is transmitted through covalent cross-links among the collagen molecules in the fibril [31]. Considering the equivalence of direct and converse piezoelectric effects, such shear deformation could produce electrical charges and build up an electric potential across the collagen fibril, which could be relevant to ion transport and cell stimulation in bone at physiological conditions. Experimental measurement has shown that when the tissue in bone is strained towards the yield point, the shear stress exerted on the surface of collagen fibrils by the extrafibrillar matrix increases and reaches a shear strength on the order of $\tau \sim 70$ MPa [37]. Collagen fibrils, depending on the position and the loading type in bone, can be subjected to different loading conditions. We particularly consider a case where a collagen fibril is under an anti-plane shear deformation with the axial shear deformations on the top and bottom half surfaces of the fibril cylinder being opposite to each other. Electric potential distribution on the fibril surface was estimated with ANSYS for a typical fibril having a diameter of 100 nm and a shear piezoelectric constant of 1 pm V^{-1}. The open circuit electrical potential difference was ∼120 mV between the top and bottom half surfaces when subjected to a shear stress of 70 MPa. Considering the fact that collagen in connective tissues are associated with the plasma membrane of cell through the basal lamina, and the inside negative potential of the cell membrane is ∼50–70 mV [13], the ability of collagen fibrils to produce an electric potential of similar magnitude implies their potential role in mechanoelectric transduction.

The ability of collagen fibrils to show piezoelectricity is expected to remain even in physiological conditions [39]. In bone, the mineral crystals of HA partially cover collagen fibrils and therefore limit water access and prevent them from swelling [39]. Studies have shown that even at 100% relative humidity, collagen in bone has only ∼12% moisture content [40]. Indeed, piezoelectricity has been measured in macroscopic samples of wet tissues albeit the piezoelectric response is quite low and decreases with increasing humidity [15, 39–41]. Under hydrated and frozen conditions (in order to create a low conductivity sample appropriate for piezoelectric measurement), tendon has been shown to be piezoelectric [41]. Some recent studies have even reported no difference in measured piezoelectric behaviors between wet and dry bone at the nanoscale [42].

4. Conclusions

In summary, individual collagen fibrils of diameters around 100 nm were isolated and studied with piezoresponse force microscopy. It was found that such collagen fibrils had unipolar axial polarizations and behaved mainly as shear piezoelectric materials having a shear piezoelectric constant of $d_{15} \sim 1$ pm V^{-1} (or pC N^{-1}). No clear local piezoelectric response was observed in the radial direction. This relatively dominant shear piezoelectric effect was the result of the quasihexagonal symmetry of the collagen fibril structure at the nanoscale. The study of piezoelectricity in nanoscopic collagen subunits and their ability to produce biologically significant electric potential in physiological conditions serves as the first step towards the eventual understanding of the evasive mechanoelectric transduction mechanism in bone remodeling and tissue growth.

[1] A collagen fibril is in fact a transversely anisotropic material. Therefore a complete and more accurate analysis will need all the related elastic moduli, shear moduli and dielectric constants in all directions. So far the data in the literature are limited, and for that matter we have modeled a collagen fibril as a linear homogeneous solid to provide us with a general estimate of the related properties, which does require adjustments as more information are available in the future.

Acknowledgments

This work was supported by National Science Foundation (Grant numbers: CMMI-0600583 and CMMI-0731096).

References

[1] Fukada E and Yasuda I 1957 On the piezoelectric effect of bone *J. Phys. Soc. Japan* **12** 1158–62
[2] Fukada E and Yasuda I 1964 Piezoelectric effects in collagen *Japan. J. Appl. Phys.* **3** 117–21
[3] Shamos M H and Lavine L S 1967 Piezoelectricity as a fundamental property of biological tissues *Nature* **21** 267–9
[4] Martin A J P 1941 Tribo-electricity in wool and hair *Proc. Phys. Soc.* **53** 186–9
[5] Marino A A and Becker R O 1970 Piezoelectric effect and growth control in bone *Nature* **228** 473–4
[6] Bassett C A L, Pawluk R J and Becker R O 1964 Effects of electric currents on bone *in vivo Nature* **204** 652–4
[7] Shamos M H, Lavine L S and Shamos M I 1963 Piezoelectric effect in bone *Nature* **197** 81
[8] Kryszewski M 2004 Fifty years of study of the piezoelectric properties of macromolecular structural biological materials *Acta Phys. Pol.* A **105** 389–408
[9] Cowin S C 2001 *Bone Mechanics Handbook* 2nd edn (New York: CRC Press)
[10] Kalinin S and Gruverman A 2007 Electromechanical behavior in biological systems at the nanoscale *Scanning Probe Microscopy* (New York: Springer)
[11] Marino A A, Becker R O and Soderholm S C 1971 Origin of the piezoelectric effect in bone *Calcif. Tissue Res.* **8** 177–80
[12] Hay E D 1991 *Cell Biology of Extracellular Matrix* 2nd edn (New York: Plenum)
[13] Lodish H, Berk A and Matsudaira P 2004 *Molecular Cell Biology* 5th edn (New York: Freeman)
[14] Kalinin S V, Rodrigueza B J, Shin J, Jesse S, Grichko V, Thundat T, Baddorf A P and Gruverman A 2006 Bioelectromechanical imaging by scanning probe microscopy: Galvani's experiment at the nanoscale *Ultramicroscopy* **106** 334–40
[15] Netto T G and Zimmerman R L 1975 Effect of water on piezoelectricity in bone and collagen *Biophys. J.* **15** 573–6
[16] Goes J C, Figueiro S D, De Pavia J A C and Sombra A S B 1999 Piezoelectric and dielectric properties of collagen films *Phys. Status Solidi* **176** 1077–83
[17] Kalinin S V, Rodriguez B J, Jesse S, Thundat T and Gruverman A 2005 Electromechanical imaging of biological systems with sub-10 nm resolution *Appl. Phys. Lett.* **87** 053901
[18] Rodriguez B J, Kalinin S V, Shin J, Jesse S, Grichko V, Thundat T, Baddorf A P and Gruverman A 2006 Electromechanical imaging of biomaterials by scanning probe microscopy *J. Struct. Biol.* **153** 151–9
[19] Marino A A and Gross B D 1989 Piezoelectricity in cementum, dentine, and bone *Arch. Oral Biol.* **34** 507–9
[20] Tanzer M L 1973 Cross-linking of collagen *Science* **180** 561–6
[21] Guthner P and Dransfeld K 1992 Local polling of ferroelectric polymers by scanning force microscopy *Appl. Phys. Lett.* **61** 1137–9
[22] Kolosov O, Gruverman A, Hatano J, Takahashi K and Tokumoto H 1995 Nanoscale visualization and control of ferroelectric domains by atomic force microscopy *Phys. Rev. Lett.* **74** 4309–12
[23] Gruverman A, Auciello O and Tokumoto H 1998 Imaging and control of domain structures in ferroelectric thin films via scanning force microscopy *Annu. Rev. Mater. Sci.* **28** 101–23
[24] Alex M and Gruverman A 2004 *Nanoscale Characterization of Ferroelectric Materials: Scanning Probe Microscopy Approach* (New York: Springer)
[25] Yang L, van der Werf K O, Koopman B F J M, Subramaniam V, Bennink M L, Dijkstra P J and Feijen J 2007 Micromechanical bending of single collagen fibrils using atomic force microscopy *J. Biomed. Mater. Res.* A **82** 160–8
[26] Peter F, Rudiger A, Szot K, Waser R and Reichenberg B 2006 Sample–tip interaction of piezoresponse force microscopy in ferroelectric nanostructures *IEEE Trans. Ultrason. Ferroelectr. Freq. Control* **53** 2253–60
[27] Peter F, Rudiger A, Waser W and Szot K 2005 Comparison of in-plane and out-of-plane optical amplification in AFM measurements *Rev. Sci. Instrum.* **76** 046101
[28] Sarid D 1994 *Scanning Force Microscopy: With Applications to Electric, Magnetic and Atomic Forces* (New York: Oxford University Press)
[29] Newnham R E, Sundar V, Yimnirum R, Su J and Zhang Q M 1997 Electrostriction: nonlinear electromechanical coupling in solid dielectrics *J. Phys. Chem.* B **101** 10141–50
[30] Kadler K E, Holmes D F, Ttotter J A and Chapman J A 1996 Collagen fibril formation *Biochem. J.* **316** 1–11
[31] Orgel J P R O, Irving T C, Miller A and Wess T J 2006 Microfibrillar structure of type I collagen *in situ* *Proc. Natl Acad. Sci.* **103** 9001–5
[32] Gutsmann T, Fantner G E, Kindt J H, Venturoni M, Danielsen S and Hansma P K 2004 Force spectroscopy of collagen fibers to investigate their mechanical properties and structural organization *Biophys. J.* **86** 3186–93
[33] Newnham R E 2005 *Properties of Materials, Anisotropy, Symmetry, Structure* (New York: Oxford University Press)
[34] Tomaselli V P and Shamos M H 1973 Electrical properties of hydrated collagen. I. Dielectric properties *Biopolymers* **12** 353–66
[35] Wenger M P E, Bozec L, Horton M A and Mesquida P 2007 Mechanical properties of collagen fibrils *Biophys. J.* **93** 1255–63
[36] Rodriguez B J, Kalinin S V, Shin J, Jesse S, Grichko V, Thundat T, Baddorf A P and Gruverman A 2006 Electromechanical imaging of biomaterials by scanning probe microscopy *J. Struct. Biol.* **153** 151–9
[37] Gupta H S, Wagermaier W, Zickler G A, Aroush D R B, Funari S S, Roschger P, Wagner H D and Fratzl P 2005 Nanoscale deformation mechanisms in bone *Nano Lett.* **5** 2108–11
[38] Gupta H S, Seto J, Wagermaier W, Zaslansky P, Boesecke P and Fratzl P 2006 Cooperative deformation of mineral and collagen in bone at the nanoscale *Proc. Natl Acad. Sci.* **103** 17741–6
[39] Anderson J C and Eriksson C P 1970 Piezoelectric properties of dry and wet bone *Nature* **227** 491–2
[40] Reinish G B and Nowick A S 1975 Piezoelectric properties of bone as functions of moisture content *Nature* **253** 626–7
[41] Marino A A and Becker R O 1975 Piezoelectricity in hydrated frozen bone and tendon *Nature* **253** 627–8
[42] Halperin C, Mutchnik S, Agronin A, Molotskii M, Urenski P, Salai M and Rosenman G 2004 Piezoelectric effect in human bones studies in nanometer scale *Nano Lett.* **4** 1253–6